Journal of Clinical Case Reports

Case Report Open Access

Pediatric Osteo-Lymphoma: A Literature Review and Case Study

Wang F[1], Altine B[2,3], Cheng C[4], Peng X[1], Lan X[2,3], Zhang Y[2,3] and Shao J[1]*

[1]*Medical imaging Center, Wuhan Children's Hospital (Maternal and Child Healthcare Hospital), Tongji Medical College, Huazhong University of Science and Technology, P.R. China*
[2]*Department of Nuclear Medicine, Union Hospital, Tongji Medical College, Huazhong University of Science and Technology, Wuhan 430022, P.R. China*
[3]*Hubei Province Key Laboratory of Molecular Imaging, Wuhan 430022, P.R. China*
[4]*Department of Radiology, Wuhan Number 6 Hospital, P.R. China*

Abstract

Background: Osteo-Lymphoma is a bone tumor that could be found in children. The world health organization (WHO) has defined Osteo-Lymphoma as lymphoma that affect only bones without the involvement of soft tissue organs. Osteo-Lymphoma is very rarely found lymphoma in pediatric patients and accounts for about 3% to 7% of bone malignancies and 4% to 5% of extranodal lymphomas. The aim of this study was to review bone lymphoma of pediatric patient, and to report Osteo-Lymphoma case diagnosed in imaging department of our hospital including Single Photon Emission Computed Tomography/Computed Tomography (SPECT/CT).

Case presentation: A 6-year-10-month old Chinese male (weight: 25 Kg, height: 120 cm) was admitted to our hospital for 2 months' bilateral lower extremities pain. He had more aggravated pain in both elbows lately associated with 15 days' headache. This patient underwent for different investigations including imaging. The imaging investigations have found multiple Osteo-Lymphoma and soft tissue tumors on forehead and right parietal bone. In addition, differential diagnosis cases from our data base were also presented and compared. The patient underwent surgery for the removal of forehead and right parietal tumors. The samples of the resected tumors were sent for immunohistochemistry analysis that confirmed the diagnosis as B cells lymphoma. Therefore, the patient was treated on the hospital standard chemotherapy regimen that is usually used in lymphoma.

Conclusion: The patient follow-up whole body SPECT/CT and other clinical tests have revealed treatment good outcomes.

Keywords: Bone lymphoma; WHO; Imaging; SPECT/CT; CT; MRI; Bone tumors; Malignant bone tumors

Abbreviations

WHO: World Health Organization; SPECT/CT: Single Photon Emission Computed Tomography/Computed Tomography; CT: Computed Tomography; HU: Hounsfield Unit; MRI: Magnetic Resonance Imaging; PBL: Primary Bone Lymphoma; DLBCL: Diffuse Large B Cell Lymphoma; hsCRP: High-sensitivity C-reactive Protein; T1WI: T1 Weighted Image; T2WI: T2 Weighted Image; FLAIR: Fluid Attenuated Inversion Recovery; ^{99m}Tc-MDP: Technetium Methylene Diphosphonates; MBq: Mega Becquerel; mCi: Milli-Curie; LCH: Langerhans Cells Histiocytosis; CD: Cluster of Differentiation; Bcl-2: B-Cell Lymphoma-2; TdT: Terminal deoxynucleotidyl Transferase; MYOG: Myogenin; MPO: Myeloperoxidase; Pax-5: B cell specific activator protein; PET/CT: Positron Emission Tomography/Computed Tomography; IL: Interleukins; TNF: Tumor Necrotic Factor; HL: Hodgkin Lymphoma; NHL: Non-Hodgkin Lymphoma; PET/MRI: Positron Emission Tomography/Magnetic Resonance Imaging

Introduction

Lymphomas are caused by lymphatic cells abnormal morphological changes and proliferation. They were described in 1832 as being malignant tumors that derived from lymphatic cells. Two forms of lymphomas were lately described. These are B- and T-cells lymphomas which were found to occur in all the systems of human body. The World Health Organization (WHO) has defined and classified lymphomas [1,2]. This hematopoietic tumor can affect both adults and infants in both genders, but primary Osteo-Lymphoma is rarely found in children. Primary Osteo-Lymphoma is described to be found in different bones of human skeleton, bone marrow and/or other tissues within the periods of symptomatic onset [3-8]. This type of lymphoma is extremely rare [9,10], and were firstly found by Parker and Jackson.

Clinical imaging has always shown its importance in the diagnosis of bone lesions including malignant tumors such as lymphomas. There is no formal agreement on the assessment of pediatric bone lymphomas [11]. Nevertheless, here we present a new case of primary Osteo-Lymphoma that has been diagnosed from pediatric patient in our hospital. The clinical, biochemical, imaging and pathological findings of this case are reported. In addition, the treatment method, the following-up imaging, and the routine biochemical results were also discussed. Our goal is to show the sensitivity of whole-body Single Positron Emission Computed Tomography/Computed Tomography (SPECT/CT) in assessment of this rarely pediatric bone lymphoma. Moreover, compare this nuclear medicine modality to Computed Tomography (CT), and Magnetic Resonance Imaging (MRI), in the assessment of this case. Differential diagnosis cases were briefly reported. Also, the patient underwent to multiple radiological bone X-Ray which was not reported here.

Semiology and epidemiology of pediatric osteo-lymphoma

Primary Bone Lymphoma (PBL), recently called osteolymphoma [12-14] is a rare extranodal malignant lymphoma that originates from the bone marrow and limited to bones. It accounts for about 3% to 7% of bone malignancies and 4% to 5% of extranodal lymphomas [3-10]. The

***Corresponding author:** Shao J, Medical Imaging Center, Wuhan Children's Hospital (Maternal and Child Healthcare Hospital), Tongji Medical College, Huazhong University of Science and Technology, P.R. China, Tel: +86 2787542457; E-mail: sw1124832019@163.com

Received December 06, 2019; **Accepted** December 18, 2019; **Published** December 26, 2019

Citation: Wang F, Altine B, Cheng C, Peng X, Lan X, et al. (2019) Pediatric Osteo-Lymphoma: A Literature Review and Case Study. J Clin Case Rep 9: 1306

average age of a person to get osteolymphoma is 40 years with incidence rate for male and female of respectively 1.2 and 1-1.6; however, it is very rarely found in children [3,15-18]. This disease was believed to originate from endothelial reticulum system. In 2002, WHO classified bone lymphoma as affected single site of the bone cortex which might involve the regional lymph nodes, or multiple bones? In addition, it defined the bone lymphoma without visceral organ involvement or regional lymph nodes as osteolymphoma. This type of lymphoma was classified as derived from malignant lymphocyte from 2013 WHO classification. It was described as a single or multiple lesions without any upper lymph nodes drainage or extranodal involvement. According to this standard classification, the bone lymphoma that might have lymph nodes drainage or extranodal involvement but no other extranodal lesions are also defined as osteolymphoma. This bone lymphoma is encountered as Diffuse Large B Cell Lymphoma (DLBCL) [10]. Therefore, in a retrospective study by Horsman, et at. 70% of cases were found to be DLBCL subtypes [5].

Case Report

A 6-year-10-month old male (weight: 25 Kg, height: 120 cm) was admitted to our hospital for 2 months' bilateral lower extremities pain. He had more aggravated pain in both elbows lately associated with 15 days' headache. During previous 2-3 months, the patient has no lower limbs pain or other obvious symptoms such as fever, rash, cough, vomiting and diarrhea which might need special care. However, before 15 days of his symptoms, he had episodes of headache and difficulty of walking but with well joints movements. In addition, the physical examination revealed an acute face, and palpable left pre-auricular solid lymph nodes. No other symptoms including mental status, appetite lost, sleepless, and voiding problems were found. He was born on a full-term cesarean section without any special health abnormality. By the request of his outpatient doctor, the patient underwent more clinical investigations to find out about his abnormal underline's conditions.

Biochemistry routine blood analysis

The routine blood test results at the patient arrival to outpatient have shown high **e**rythrocytes 5.29 × 10^{12}/L; platelets 337 × 10^{9}/L; increased eosinophils percentage and total count: respectively 28.8% (normal range: 0.5-5%); and 1.81 × 10^{9}/L (normal range: (0.05-0.5) × 10^{9}/L). A slight morphological change of erythrocytes was also observed. The white blood cells presented heterotypic lymphocytes and increase eosinophils ratio. Other additional tests were run including the liver, the renal functions, and the electrolytes evaluations, the myocardial zymogram and the blood amylase tests which have shown normal findings. In addition, the tumor marker High-sensitivity C-Reactive Protein (hsCRP) evaluation was normal (11.20 mg/L), therefore no inflammation was shown. The cerebrospinal fluid analysis has shown positive glucose intake and decreased proteins level (0.12 g/L) but normal chlorides (Cl. 118.3 mM/L), and glutamates (3.70 mM/L). However, no neoplastic cells phenotype was observable but higher proportion of eosinophils was found from this patient bone marrow biopsy.

Imaging evaluations

The physical examination of acute face was evaluated with CT scan of the head which revealed frontal and parietal bones mass lesions. The CT shows epidural hyper-dense ellipsoid-round large soft tissue lesions protruded more externally to the scalp from the frontal bone and internally from parietal bone. The forehead lesion appeared as a homogeneous density mass and measured: 3.1 cm × 2 cm × 3.4 cm (left and right diameter × front and rear diameter × upper and lower diameter). The corresponded Hounsfield Unit (HU) of the forehead extra-epidural soft tissue was 55, and greater than the other proximal soft tissue density. The parietal lesion was also homogeneously dense and measured: 1.7 cm × 1.8 cm × 1.6 cm (left and right diameter × front and back diameter × upper and lower diameter). In addition, the right parietal plate appeared as mildly widen heterogeneous density with irregular region of bone destruction and cortical discontinuity. An internal slight shift of the adjacent brain tissue caused by the mass, and a mild decrease left occipital bone density was observed. Moreover, an enlarged left pre-auricular lymph node was identified which measured approximately 0.7 cm to 1.4 cm with HU of 38. No other mass lesions were found in the brain parenchyma.

These tumors appeared as mild iso-intensity and hyper-intensity signals on MRI respectively T1 weighted (T1WI) and T2 weighted images. The fluid attenuated inversion recovery (FLAIR) T2 sequence has shown homogeneous higher hyper-intensity signal tumors. Additionally, the enhanced images acquisition has shown moderate homogeneous enhancement. The final MRI diagnosis referred these mass lesions as probable tumor without stated whether benign or malignant (Figures 1a-1h). As suspected tumors was found with previous CT and MRI assessment, the patient underwent to technetium-methylene diphosphonates (^{99m}Tc-MDP, a dosage proportional to the patient weight, approximately 250 MBq= 6.76 mCi) whole body SPECT/CT evaluation of the skeleton. Therefore, diffuse hot spots regions were found on the right parietal bone, left distal radius, and bilateral talus bones, calcaneus, navicular, tarsi, cuneiforms (medial, middle and lateral) and the five metatarsal bones. These have shown the metabolic features of the tumors spread to the bones then a diagnosis of malignant tumors was made at the nuclear medicine department.

In addition, to assess more on lower limb pain presented by the patient, bilateral distal tibia including the ankles SPECT/CT and CT scans were performed. This has shown abnormal coarse cortical densities on CT of left distal tibia metaphysis with localized "worm-shaped" bone destruction. The anterior and the posterior SPECT images has revealed abnormal radiotracer metabolism. Moreover, this were observed on fused images as hot spot corresponding to radiotracer metabolic lesion and confirmed as bone lymphoma (Figures 2a and 2b).

Differential diagnosis

The frontal and right parietal bone tumors and additional bone lesions found from this patient seems to be differentiate with three malignant diseases. First, neuroblastoma with multiple bones metastases which is commonly observed as solid tumor in children [19] under 5 years of age, and 2/3 of this malignancy is commonly localized on the adrenal medullar gland [20]. The advanced form of neuroblastoma represents 40% to 70% of malignant tumor with distant metastases most likely in the bones, the liver, the epidural etc. but rarely involves the lung. Its early bone metastasis appeared as coarse and irregular trabeculae, subsequently with mild hyperplasic destructive bones. The typical CT and MRI finding of neuroblastoma bone metastasis are most likely like that of osteo-lymploma. The metastatic bone destruction pattern is the differential diagnosis of neuroblastoma bone metastases from osteo-lymploma. The high grade of malignant tumors metastases would highly result on whole body SPECT/CT as hot spot bone metastases (Figures 3a-3f).

The Langerhans Cell Histiocytosis (LCH) is the second differentiate lesion to osteo-lymploma. Its clinical symptoms are mainly fever, rash and accompanying by hepatosplenomegaly. This disease can be seen

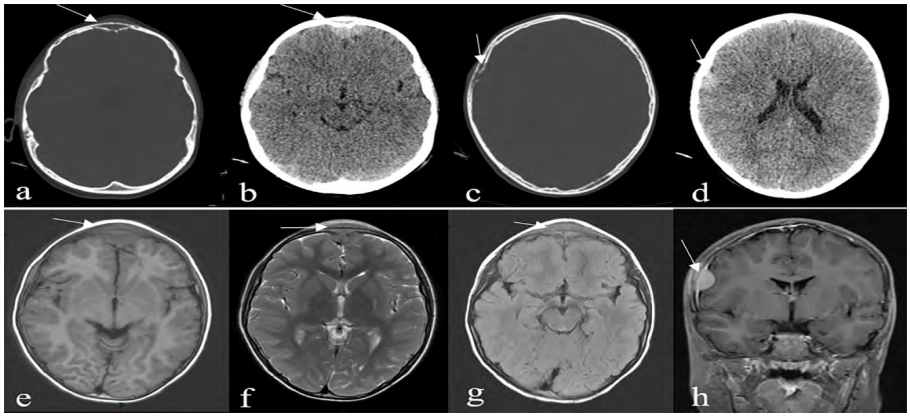

Figure 1: (a-h) Osteo-Lymphoma on forehead and right parietal bones found on plain CT and MRI scans. Upper panel, a and b show homogeneous density forehead tumor with cortical destruction (axial bone window, arrow) which is hyper-dense on axial soft tissue window (b, arrow) with shadowing effect on the adjacent brain parenchyma. The tumor effect can be observed exteriorly to the scalp. Additionally, homogeneous density on the right parietal plate is detected on c and c (respectively axial bone and soft tissue windows. Arrows) with cortical destruction. Lower panel, e, f and g are axial MRI T1WI, T2WI and FLAIR showing the forehead tumor as respectively mild iso-intensity, hyperintensity and high hyperintensity patterns (arrows). In addition, the right parietal lesion on H has shown coronal T1WI homogeneous enhancement (arrow). No lesion was found on the brain parenchyma.

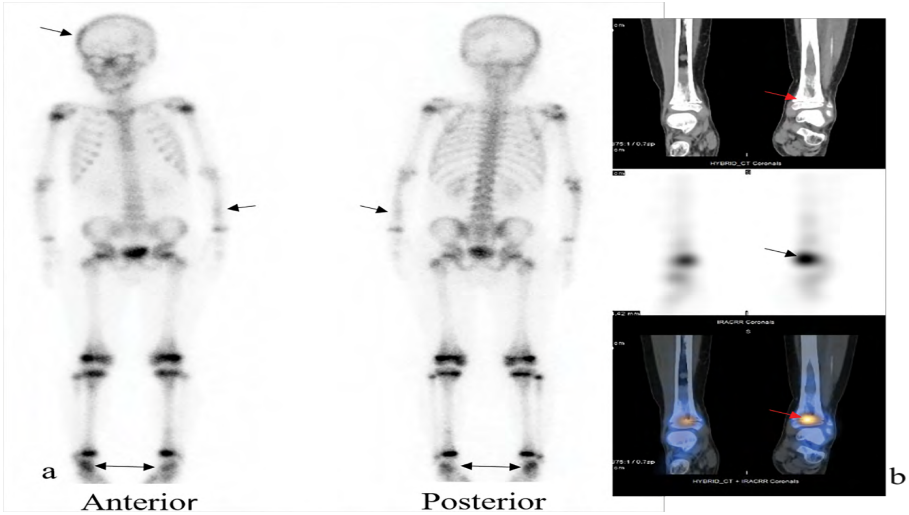

Figure 2: (a and b) Represents the whole-body bone scan (anterior and posterior views) and tomographic SPECT/CT images. A. shows the anterior and posterior bones with abnormal hot spots on the right parietal bone, left distal radius, and bilateral talus, calcaneus, navicular, tarsi, cuneiforms (medial, middle and lateral) and the five metatarsal bones. These hot spots are shown by the arrows on (a) and (b) above image shows CT of bilateral tibia with hyper-density lesion detected on the left distal tibia metaphysis (red arrow). This lesion is shown by tomographic SPECT and fused images (respectively middle and below images) where localized hot spot area on the right distal tibia is observed (black and red arrow).

on new born babies, children and adolescents between the age of 5-10 years. It is also found to be very severe clinical condition that affect different system of the body [21]. The CT and MRI patterns of this disease can be identical to osteo-lymploma such as the cortical mild expansion, predominantly with destructive bone. The MRI of LCH shows hypo-intensity T1WI, hyper-intensity T2WI signals, and a moderate homogeneous iso-intensity or soft tissues mass enhancement significantly without intra-cystic changes. The metastatic bone destruction pattern is the differentiation of this malignant disease from osteo-lymploma. Therefore, LCH tend to show a diffuse or localize hot spot-on whole-body bone scan and SPECT/CT fused acquisition (Figures 4a-4f).

The third most likely disease that could be differentiate from this case is Ewing's sarcoma. This bone tumor is one of the highest-grade malignant disease commonly found during childhood. The incidence of sarcoma is most likely the osteosarcoma which happens in children and adolescents of age between 10-20 years [22,23] more frequent in male. In addition, it affects mostly long bones including the femur, the tibiofibular and the humerus. However, it can occur on the skull, including on the mandibular and on the pelvis flat bones [23]. The imaging features are characterized by an onion outer layer like lesion, a stratiform periosteal reaction, and an erosion bone with predominant osteolitic destruction. Similarly, to advance neuroblastoma bone metastasis, LCH, and Ewing sarcoma CT and MRI T1WI and T2WI

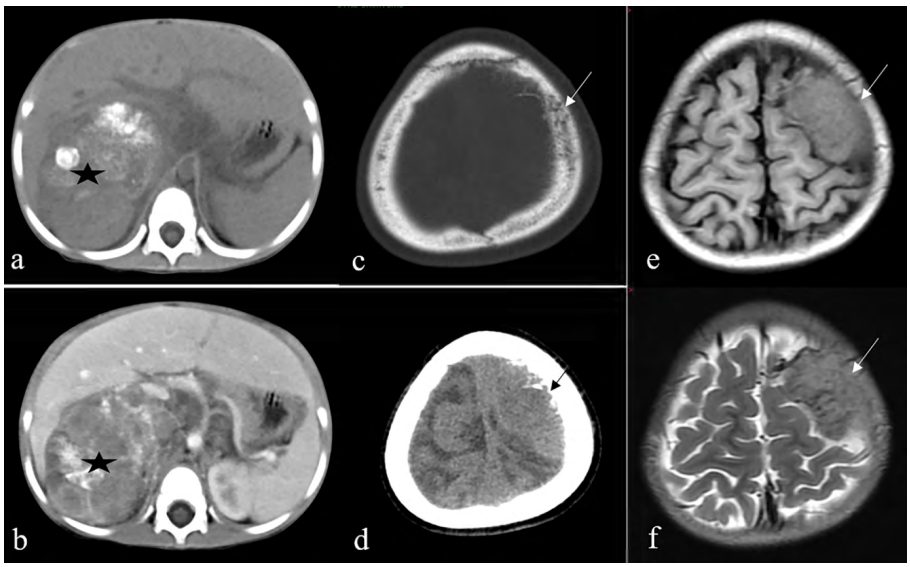

Figure 3: (a-f) Neuroblastoma of 2 year-2 month-old female with metastasis on the left parietal bone. a and b are upper abdominal CT scan taken 1 month before the head scans showing the original tumor with heterogeneous enhancement (black asterisks). c and d are bone and soft tissue windows where the left parietal density metastasis is visualized (arrows). e and f show the same metastasis respectively on axial MRI T1WI and T2WI as iso-intensity lesion (arrows).

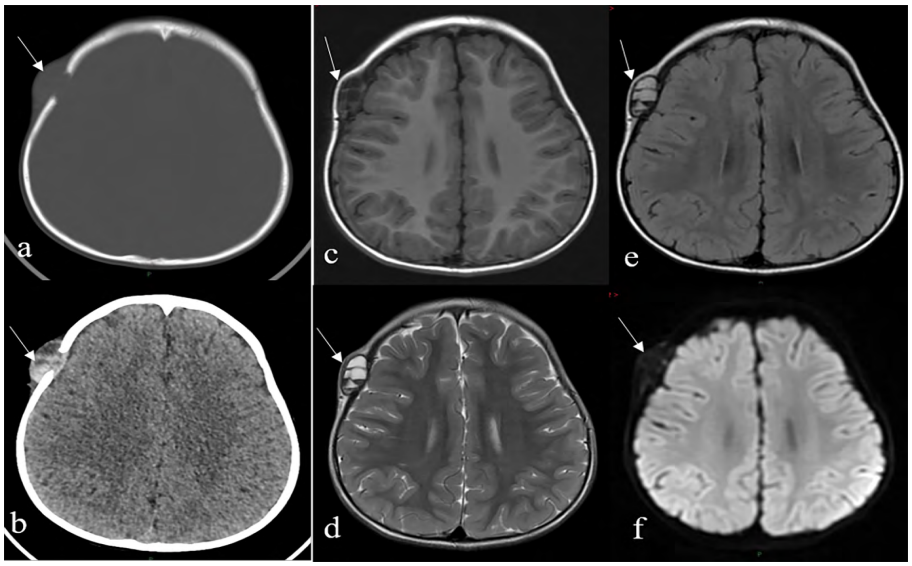

Figure 4: (a-f) 2 year-7 month-old male with Langerhans Cell Histiocitosis (LCH) on multiples areas of his body but only the head lesion is shown here. a and b are axial bone and soft tissue windows CT where left parietal bone destructed iso-density cystic lesion that extends to the coronal suture toward the frontal bone is visualized (arrows). In addition, the lesion is shown on MRI as well circumscribed cystic hypo-intense on c axial T1WI, hyper-intense on d axial T2WI, iso-intense one FlAIR, and hypo-intense on f DWI (arrows).

are most likely to osteo-lymploma patterns (Figures 5a-5d). In addition, other imaging features can be found but depending on the muli-modality technics that are used to assess this tumor. As example, SPECT/CT can also be used to evaluate Ewing sarcoma specially to find bone metastasis anywhere on the skeleton. Moreover, Ewing sarcoma sensitivity to radiotherapy helps to differentiate other bone lesion, though the final decision still relies on the pathological and the immuno-histochemical evaluation.

Tumor resection, Immunohistochemistry and Biopsy examinations

Based on the physical and the clinical diagnosis findings, the forehead and the right parietal tumors of this patient were removed from surgery. At the opening of the regional skull, a significant tumor erosion of the epidural and a thicken dura matter connected white tissues were characterized. The anatomical structures

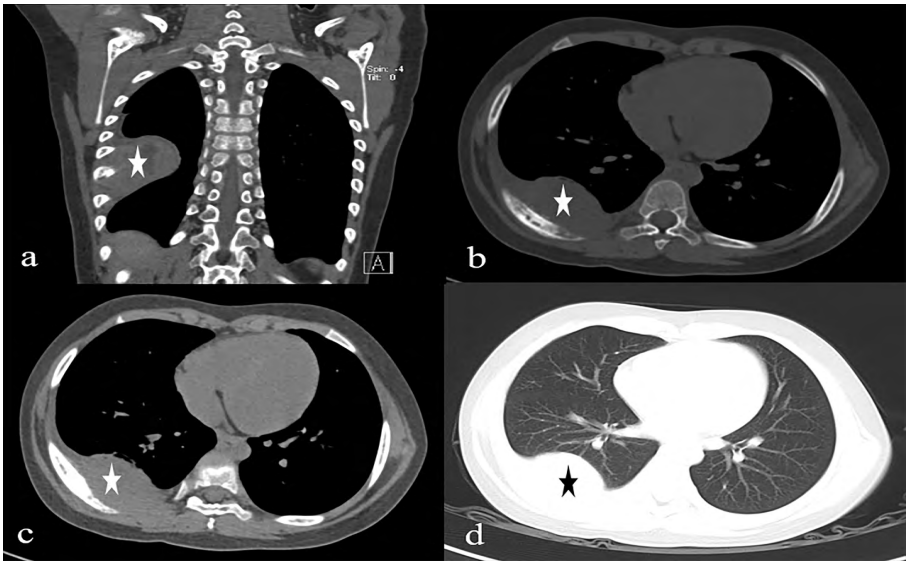

Figure 5: (a-d): 8year-old male, Ewing sarcoma on the right lung pleura. (a) coronal bone window CT shows an iso-density pleural and extra-pleural tumor originated from the contralateral rib and extents to the middle right lobe (white asterisk). A contralateral rib cortical destruction patterns are observed on axial bone window on b caused by the tumor (arrow and white asterisk). On axial soft tissue window c, a contralateral rib hyper-density is also shown with the extension of the tumor to the lung (white asterisk), however the lung window CT d, shows a smooth interface on the lung parenchyma (black asterisk).

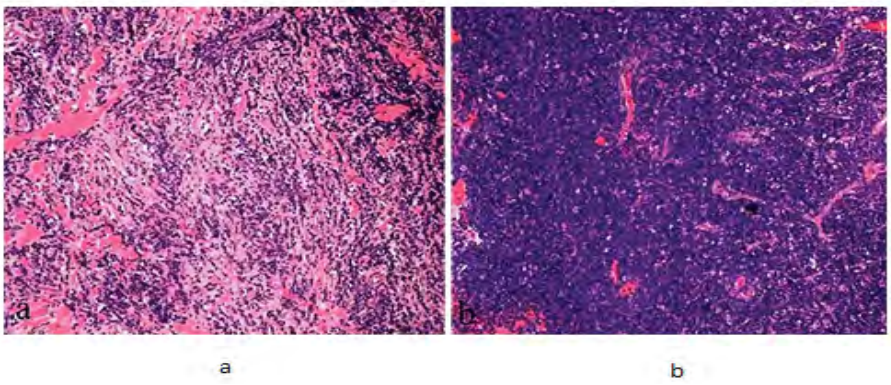

Figure 6: (a and b) (Scalp, calvarium and dura matter) B Lymphoblastic lymphoma found immunohistochemistry on the resected tumors (a and b).

including the scalp and dura matter tissue was appreciated by naked eyes. The immunohistochemistry analysis of the tumor tissue was performed Figures 6a and 6b. Therefore, the assessment of Cluster Of Differentiation (CD) markers and other biological markers such as B-cell lymphoma-2 (Bcl-2), Terminal deoxynucleotidyl Transferase (TdT), Myogenin (MYOG), Myeloperoxidase (MPO) genes, also the B cell specific activator protein (Pax-5) were performed to make a final diagnosis and to specify the type of tumor cells that are involved. A negative CD3 (-), positive Bcl-2 (+), positive TdT (+), negative Myogenin (-), negative CD20 (-), negative Bcl-6 (-), negative CD21 (-), positive CD10 (+), negative CD5 (-), positive CD99 (+), negative MPO (-), negative Granz B (-), Ki-67 (index 80%), and positive Pax-5 (+) were found. Finally, the diagnosis of the tumors from this pediatric patient was confirmed as B-cell lymphoblastic lymphoma.

Treatment and clinical follow-up

The pathological final diagnosis of B-cells lymphoblastic lymphoma after resection from this patient was treated following the LBL-2016 chemotherapy guidelines which are routinely used in our hospital. At completion of a year of treatment, the patient face appeared normal, without any abnormal features. In addition, the follow-up full immune test, liver and renal functions have shown normal features. Moreover, the control Whole body SPECT/CT performed 4 months and 11 months after treatments has shown better outcomes compare to the previous found bone lesions (Figures 7a and 7b).

Discussion

Primary pediatric bone lymphoma diagnosis is very rare made in nuclear medicine. However, here the diagnosis of Osteo-Lymphoma was accomplished. The physical examination and laboratory tests may be useful on the diagnosis of this malignant disease. Increased erythrocyte may be identified [16]. The gold standard medical diagnostic tool of PBL is immuno-histochemical examination [24,25]. It is very important to evaluate a patient with any physical symptoms by

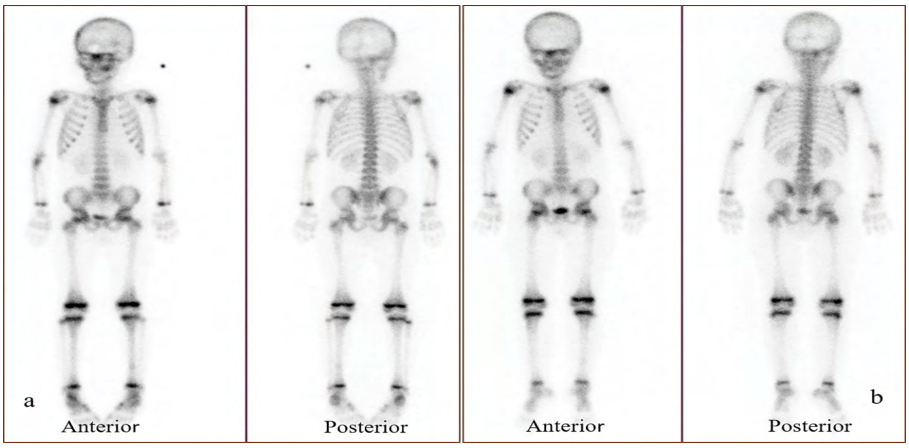

Figure 7: (a and b) Represents the whole-body bone scan (anterior and posterior views) of the patient follow-up after treatment. On the right, 4 months after treatment (a) shows well distribution of 99mTc-MDP with a remaining hot spot on the right parietal bone that represents the surgical intervention area. On the left is 11 months after treatment (b) where anterior (right) and posterior (left) shows well distribution tracer without any abnormality that confirmed the treatment effectiveness.

conventional examinations. Radiographic finding of bone lymphoma be sclerotic, osteolytic, and radiolucent area surrounded by non-calcify soft tissue mass [12,26]. In addition, both CT and MRI are important imaging modalities that have shown their sensitivities to lymphomas. They have shown useful findings in assessment of PBL. The CT can clearly show the extend of bone damage, though it has limitations to determine the expansion of lesions which may occur in the pia- matter and the brain parenchyma. The MRI has shown high sensitivity in that regard and more soft tissue lesion can be diagnose which may involve the meningeal and the parenchymal lesions. Therefore, it is more recommended in suspected neurological and other soft tissue diseases.

In our presented case, whole body ^{99m}Tc-MDP SPECT/CT helps to show the metabolism of the right parietal bone tumors and it also found additional bone lesions. The CT of the head performed on a single CT machine discovered the skull lesions but did not found other disease because only a regional CT was performed to ovoid more radiation exposure. Although, the SPECT/CT also uses radiation but a small intra-veins dose according to the weight of the patient is injected, and the CT scan of this fused machine is only done when a suspected unclear anatomic lesion is seen in specific part of the skeleton. Therefore, the whole-body SPECT/CT images have shown high sensitivities in the assessment of this case. This imaging modality has an advantage of showing the whole anatomical skeleton and physiological features of the bones. Moreover, the posterior, the anterior views and multiple fused SPECT and CT planar images provide more information in metabolic evaluation of bones including in this case. This help to improve the accuracy of imaging diagnosis of malignant bone tumors and metastases. They have brought changes in the historical single modalities lack of malignant tumors evaluation and improved the specificities of imaging diagnosis.

Bone scintigraphy such as ^{99m}Tc-MDP SPECT or SPECT/CT is usually performed to identify metastases that can occur during clinical follow-up of primary cancers. However, in absence of Positron Emission Tomography/Computed Tomography (PET/CT), bone SPECT/CT can be used for the staging of bone lymphoma.

Osteo-Lymphoma cells caused the increase production of Interleukins (IL) 21, IL26 and Tumor Necrotic Factor (TNF) cytokines which induced bone fracture features. Therefore, this induces the formation of small cortical neoplastic pattern. In addition, widespread destruction of the bone cortex might occur. The specific feature of Osteo-Lymphoma is the unrelated cortical destruction by the soft tissue tumor. In most cases, they are Non-Hodgkin lymphoma (NHL) were the commonly pathologically seen is diffuse large B-cell lymphoma. The Hodgkin lymphoma (HD) type is less likely seen. Osteo-Lymphoma has clinical non-specific pattern and the early diagnosis is more complicated.

Bone tumors commonly occur on the skull, the spine, the pelvis, the femurs, and the tibia. The imaging characteristics are not specific, however osteolytic destructions are the most observable pattern including patchy or worm-like appearances with fuzzy or blur boundaries which might have periosteal reactions more likely in the long bones. The cortical destruction is seen with surrounding soft tissue tumefaction. On CT scan they are homogeneous mild hyperdense; MRI T1WI, T2WI and FLAIR show homogeneous is intensity signals. The enhanced MRI scan shows a mild to moderate enhancement. These features are specific imaging patterns of Osteo-Lymphoma.

The imaging evaluation of presented case whole body has shown frontal and right parietal dura matter lesions and additional distal tibia lesion. Although, MRI has shown better obvious bone marrow lesions and the tumor compared to X-Ray and CT scan. However, CT found better degree of cortical bone destruction than MRI but both CT and MRI were less sensitive to determine the whole-body lesions compared to whole body SPECT/CT. The SPECT/CT was able to show not only the cortical bone lesions but also simultaneously shows tomographic lesions alone with the CT. The CT fused to SPECT helps for precise anatomical localization of the lesions, boundaries, and sizes; additionally, fused images of SPECT and CT are used for quantitative and qualitative metabolic appreciation. Despite, certain limitations of differentiation of some malignant tumors in this case such as bone metastatic neuroblastoma, LCH and Ewing sarcoma, the whole-body SPECT/CT have shown to be very important in the skeleton assessment of Osteo-Lymphoma. However, other multi-modalities imaging such as PET/CT and PET/MRI have shown to be more sensitive than SPECT/CT in assessment of bone tumors and metastasis, but their expensive costs and lack of availability make some centers to utilize SPECT/CT.

Conclusion

The imaging modalities have always shown their spots in the

evaluation of bone tumors. Here, in the diagnosis and the follow-up of this presented primary bone lymphoma, the imaging modalities have once again demonstrated their usefulness. The newly used imaging technique such as SPECT/CT has proved itself in the finding of this primary bone lymphoma and has added more in the narrative of nuclear medicine technology.

References

1. Lenz G, Staudt LM (2010) Aggressive lymphomas. New Eng J Med 362: 1417-1429.
2. Campo E, Swerdlow SH, Harris NL, Pileri S, Stein H, et al. (2011) The 2008 WHO classification of lymphoid neoplasms and beyond: Evolving concepts and practical applications. Blood 117: 5019-5032.
3. Lima FP, Bousquet M, Gomez-Brouchet A, De-Paiva GR, Amstalden EM, et al. (2008) Primary diffuse large B-cell lymphoma of bone displays preferential rearrangements of the c-MYC or BCL2 gene. Am J Clinical Pathol 129: 723-726.
4. Deshmukh C, Bakshi A, Parikh P, Nair R, Pai V, et al. (2004) Primary non-Hodgkin's lymphoma of the bone: A single institution experience. Med Oncol 21: 263-267.
5. Horsman JM, Thomas J, Hough R, Hancock BW (2006) Primary bone lymphoma: A retrospective analysis. Int J Oncol 28: 1571-1575.
6. Kitsoulis P, Vlychou M, Papoudou-Bai A, Karatzias G, Charchanti A, et al. (2006) Primary lymphomas of bone. Anticancer Res 26: 325-337.
7. Stein ME, Kuten A, Gez E, Rosenblatt KE, Drumea K, et al. (2003) Primary lymphoma of bone, A retrospective study: Experience at the Northern Israel Oncology Center (1979-2000). Oncol 64: 322-327.
8. Yuste AL, Segura A, Lopez-Tendero P, Girones R, Montalar J, et al. (2004) Primary lymphoma of bone: A clinico-pathological review and analysis of prognostic factors. Leukemia Lymph 45: 853-855.
9. Bhagavathi S, Fu K (2009) Primary bone lymphoma. Arch Pathol Laborat Med 133: 1868-1871.
10. Maruyama D, Watanabe T, Beppu Y, Kobayashi Y, Kim SW, et al. (2007) Primary bone lymphoma: A new and detailed characterization of 28 patients in a single-institution study. Japanese J Clin Oncol 37: 216-223.
11. Lones MA, Perkins SL, Sposto R, Tedeschi N, Kadin ME, et al. (2002) Non-Hodgkin's lymphoma arising in bone in children and adolescents is associated with an excellent outcome: A Children's Cancer Group report. J Clin Oncol 20: 2293-2301.
12. Mulligan ME, McRae GA, Murphey MD (1999) Imaging features of primary lymphoma of bone. Am J Roentgenol 173: 1691-1697.
13. Coley BL, Higinbotham NL, Groesbeck HP (1950) Primary reticulum-cell sarcoma of bone; summary of 37 cases. Radiol 55: 641-658.
14. Boston HC, Dahlin DC, Ivins JC, Cupps RE (1974) Malignant lymphoma (so-called reticulum cell sarcoma) of bone. Cancer 34: 1131-1137.
15. De-Leval L, Braaten KM, Ancukiewicz M, Kiggundu E, Delaney T, et al. (2003) Diffuse large B-cell lymphoma of bone: An analysis of differentiation-associated antigens with clinical correlation. Am J Surg Pathol 27: 1269-1277.
16. Haque SA, Shad A, Ozdemirli M, Shanmugam VK, Kallakury B (2009) A thirteen-year-old female with primary T-cell rich B-cell lymphoma of bone masquerading as chronic recurrent multifocal osteomyelitis. Pediat Rep 1: 3.
17. Anderson JR, Wilson JF, Jenkin DT, Meadows AT, Kersey J, et al. (1983) Childhood non-Hodgkin's lymphoma: The results of a randomized therapeutic trial comparing a 4-drug regimen (COMP) with a 10-drug regimen (LSA2-L2). New Eng J Med 308: 559-565.
18. Zhao XF, Young KH, Frank D, Goradia A, Glotzbecker MP, et al. (2007) Pediatric primary bone lymphoma-diffuse large B-cell lymphoma: Morphologic and immunohistochemical characteristics of 10 cases. Am J Clin Pathol 127: 47-54.
19. Haase GM, Perez C, Atkinson JB (1999) Current aspects of biology, risk assessment, and treatment of neuroblastoma. Sem Surg Oncol 16: 91-104.
20. Maris JM (2010) Recent advances in neuroblastoma. New Eng J Med 362: 2202-2211.
21. Buchmann L, Emami A, Wei JL (2006) Primary head and neck Langerhans cell histiocytosis in children. Otolaryngology-head and neck surgery. J Am Acad Otolaryngol Head Neck Surg 135: 312-317.
22. Vaccani JP, Forte V, De-Jong AL, Taylor G (1999) Ewing's sarcoma of the head and neck in children. Int J Pediat Otorhinolaryngol 48: 209-216.
23. Windfuhr JP (2004) Primitive neuroectodermal tumor of the head and neck: Incidence, diagnosis, and management. Ann Otol Rhinol Laryngol 113: 533-543.
24. Gianelli U, Patriarca C, Moro A, Ponzoni M, Giardini R, et al. (2002) Lymphomas of the bone: A pathological and clinical study of 54 cases. Int J Surg Pathol 10: 257-266.
25. Suryanarayan K, Shuster JJ, Donaldson SS, Hutchison RE, Murphy SB, et al. (1999) Treatment of localized primary non-Hodgkin's lymphoma of bone in children: A Pediatric Oncology Group study. J Am Soc Clin Oncol 17: 456-459.
26. Baar J, Burkes RL, Bell R, Blackstein ME, Fernandes B (1994) Primary non-Hodgkin's lymphoma of bone: A clinicopathologic study. Cancer 73: 1194-1199.